K. C. Gupta
Department of Mechanical Engineering
University of Illinois at Chicago
Chicago, Illinois 60680

On the Nature of Robot Workspace

Abstract

This paper demonstrates that workspace analysis is not merely a tool of volumetric analysis. In order to emphasize its broad implications in the configuration synthesis of robot manipulators, we use the term workspace theory. *After reviewing some recent research on robot workspaces, it is shown that workspace theory leads to an anthropological observation in biomanipulation, qualitative transformations of holes and voids (central or toroidal), the geometric inversion method for the prediction of the number of solution sets, the existence of solution transition boundaries within the workspace (dexterous or total), and the influence of joint variable limits on the workspace and the multiplicity of solution sets.*

1. Introduction

This paper presents some recent developments on robot workspaces. A clear understanding of the nature of robot workspaces leads to useful insights into the configuration synthesis of robots. The workspace $W_i(P)$ with respect to ith axis is defined as the totality of points that can be reached by the gripper point or tool tip P. The shape of the workspace is a complex solid of revolution when the first joint is revolute, and a hollow/solid prismatic shape when the first joint is prismatic. Workspace can be determined from:

1. the description of the manipulator in terms of either the parameters a_i (link length), α_i (link twist), θ_i (joint angle), or s_i (joint offset) (Denavit and Hartenberg 1955) or joint axes locations $\mathbf{Q}_{i0}$ and directions $\mathbf{u}_{i0}$ in a zero reference position (Gupta 1981): and
2. joint variable ranges.

Several methods for the determination of workspaces have been developed in Gupta and Roth (1981), Kumar and Waldron (1981), Sugimoto and Duffy (1981), Tsai and Soni (1981), Lin and Duffy (1982), Hansen (1983), Hanson, Gupta, and Kazerounian (1983), and Yang and Lee (1983).

2. Quantitative Global Evaluation

After a manipulator has been normalized, for example with respect to its maximum reach, it can be evaluated or optimized in terms of workspace volume. A comparative study of various manipulators based upon a volumetric index is given in Yang and Lee (1982).

The total workspace can be divided into primary (or dexterous) and secondary workspaces. In the *primary* (or *dexterous*) *workspace*, all tool orientations around the tool tip point P are possible. The questions of existence and determination of primary workspace are investigated in Gupta and Roth (1981) and Kumar and Waldron (1981). A common robot configuration with six degrees of freedom consists of a three-degrees-of-freedom positioning of a wrist point H, followed by a *three-roll wrist* (or equivalent configuration with three revolutes cointersecting at a wrist point). Primary workspace for such arrangements can be determined easily: first, the workspace $W_1(H)$ of the wrist point H is determined. Then a sphere of radius HP is moved with its center on the boundary of the workspace $W_1(H)$. The inner and outer envelopes are the boundaries of primary and total workspaces, respectively. Primary workspaces of several manipulator arrangements are considered in Gupta and Roth (1981).

A useful indicator of workspace quality is its *primary* (or *dexterous*) *fraction*. This fraction should be as large as possible. For manipulators with a terminal three-roll wrist, the primary workspace decreases monotonically, and the total workspace increases monotonically with an increase in hand size $h = HP$ (Gupta and Roth 1981). Hand size is taken to be the distance between the cointersection wrist point and tool tip point. For zero hand size (i.e., $HP = 0$), the

This paper was first presented at the Israel Conference on Mechanical Engineering, Haifa, Israel, in June 1984. Reprinted by permission of the *Israel Journal of Technology*, Weizman Science Press of Israel.

The financial support of the U.S. Army Research Office under the contract number 20125 EG/DAAG29-83-K0144 is gratefully acknowledged.

The International Journal of Robotics Research,
Vol. 5, No. 2, Summer 1986

Fig. 1. Kinematic wire diagram of human arm (upper) and workspace radii vs. hand size with joint J7 frozen (lower).

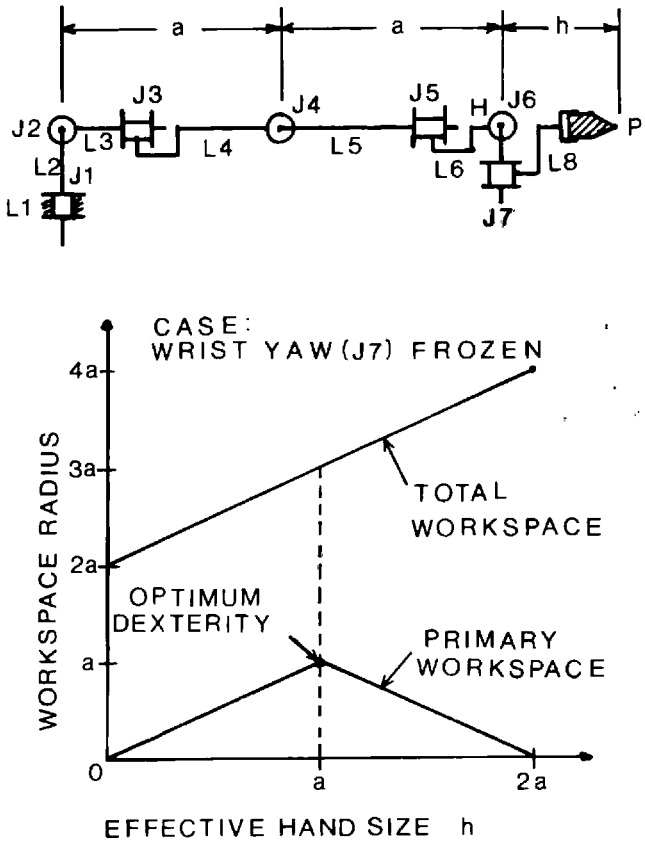

primary workspace becomes equal to the total workspace, and the fraction becomes unity. A zero hand size is impossible to achieve, however, due to hardware considerations. Therefore the hand size *HP* should be as small as possible. Examples of a three-roll wrist with three cointersecting and sequentially orthogonal revolutes with joint mounted motors are found in *Stanford Arm, Unimation Puma,* and *IBM* robots. An example of a geared three-roll wrist that represents an interesting modification of mechanical differential and uses remote joint actuators is found in *Bendix* robots (Freudenstein, Longman, and Chen 1984; Gupta 1985).

For manipulators without a terminal three-roll wrist (with the last three axes cointersecting at a point), hand size can be defined as the distance between the tool tip point and the last or next to last axis that does not pass through the tool tip. Existence of a primary (or dexterous) workspace in such cases is not insured. Also, in some cases the volume of the primary workspace has an optimum value for a finite hand size (Gupta and Roth 1981). An interesting application of this case to biomanipulation now follows.

2.1. Biomanipulation

The study of manipulation in the biological domain falls under the category of biomanipulation. Of special interest is the articulation of the human arm. Manipulators such as *Cincinnati-Milacron* T^3 and the space shuttle manipulator are patterned after human arm articulation. A *kinematic wire diagram* of the human arm (without a five-fingered hand) is shown in Fig. 1. The joints are labeled $J1, \ldots, J7$ (all revolutes). The links are labeled $L1, \ldots, L8$, with the base as the first link. Symbolically, this manipulator configuration can be represented as $R \perp R \perp R\perp R\perp R\perp R\perp R$: here R represents revolute, P represents prismatic (none present), $\parallel$ or $\perp$ means that adjacent axes are parallel or perpendicular, and the curved bar on a pair or group of joints means cointersection at a single point. A more precise mathematical description can be written, but it is not necessary for this illustration.

In Fig. 1, the shoulder is modeled as three cointersecting revolutes with shoulder yaw $J1$, pitch $J2$, and roll $J3$. The elbow is revolute $J4$. The wrist is modeled as three cointersecting revolutes with wrist roll $J5$, pitch $J6$, and yaw $J7$. All of the seven joints have partial mobility ranges. The degree of freedom with the smallest mobility range is the wrist yaw of approximately 45 degrees. The shoulder roll is about 90 degrees. The ranges of the remaining joints are approximately 180 degrees (shoulder yaw and pitch, elbow, wrist roll and pitch). The hand size h is defined as the distance between the wrist pitch axis and the finger tips (or the tool tip if a tool is gripped by the fingers).

If we now ignore the rather limited wrist yaw ($J7$) degree of freedom, we are left with a six-degrees-of-freedom manipulator without three cointersecting terminal joints. Its workspace with full mobility joints J_1, J_6 is spherical. A plot of its total and dexterous workspace radii with respect to the hand size is shown in Fig. 1. Therefore the point of optimum dexterity occurs when the following condition on three distances is satisfied: D (shoulder, elbow) = D (elbow, wrist = D (wrist, tool tip) = a. This observation also remains

valid approximately when the seventh degree of freedom of a rather limited yaw $J7$ is added. This observation is very interesting because it suggests that the conditions of optimum dexterity are nearly met when the fingers are outstretched or the hand is holding a small tool, such as a mechanic's screwdriver, an artist's brush, etc. Of course, all tools have specific functions, but whether their use optimizes dexterity or mechanical skill is an important but otherwise overlooked observation derived from the workspace theory. This may be another hidden motivation for the rapid development of tools over the course of civilization and the instinctive behavior of primates when provided with small objects.

3. Quantitative Local Evaluation

The capability of the robot is limited in the secondary workspace. However, a local analysis of several points in the secondary workspace may be done and stored for future use. Local analyses are done in terms of approach angles and approach lengths.

In the secondary workspace, only certain tool orientations are possible around the tool tip point. The possible angles of a tool axis are called *approach angles,* and their limiting values are the approach angle limits. Collectively, permissible orientations of a tool axis define a reachable solid angle about the tool tip and a *service coefficient* θ (Roth 1976) can be defined as follows: $\theta = \frac{1}{4\pi}$ (reachable solid angle). The approach angle is a useful concept in intricate assembly and nut-tightening operations where tool orientation capability in a localized zone is important.

Linear axial travel of the tool away from a tool tip point along various directions defines *approach lengths* and their limits. Approach length is a useful concept in operations such as drilling and insertion. A convenient way to present approach angle and approach length data is in terms of *ray graphs* in two planes (Hansen 1983). The ray graphs for a point P in the primary (or dexterous) workspace are shown in Fig. 2. This point can be approached from all directions. The tool can be moved axially from a point on the solid boundary to point P. This particular set of ray graphs shows that approaches to point P from the right are rather restricted. The ray graphs for a point in the secondary workspace are shown in Fig. 3. In this case, the point cannot be approached at all from the right. The boundary of the ray graph now contains the point P as a cusp. This cusp provides the approach angle limits at point P.

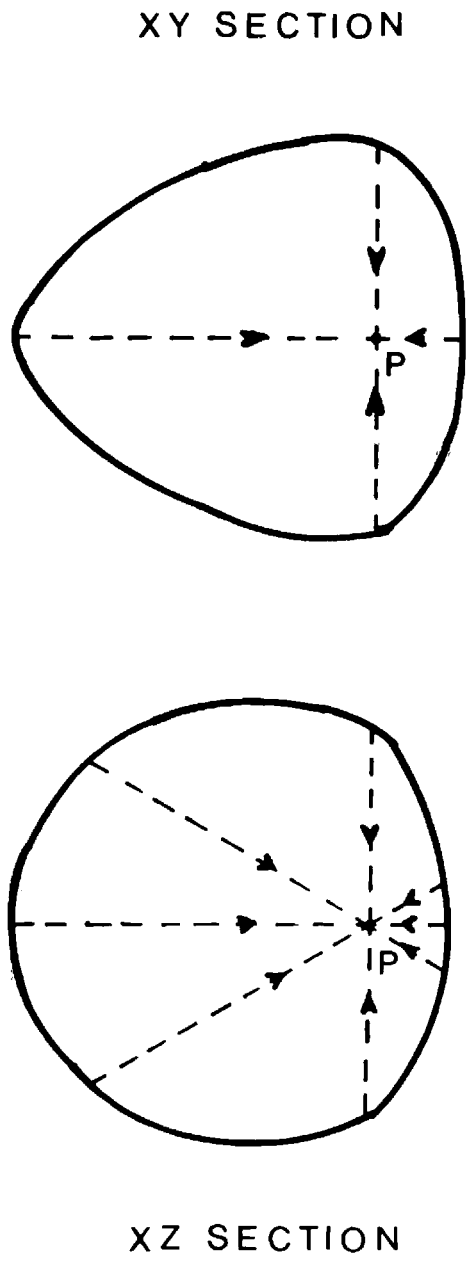

Fig. 2. XY and XZ sections of the approach length ray graphs for a point P in the primary workspace. Z axis is the vertical base column axis.

Fig. 3. XY and XZ sections of the approach length ray graphs for a point P in the secondary workspace.

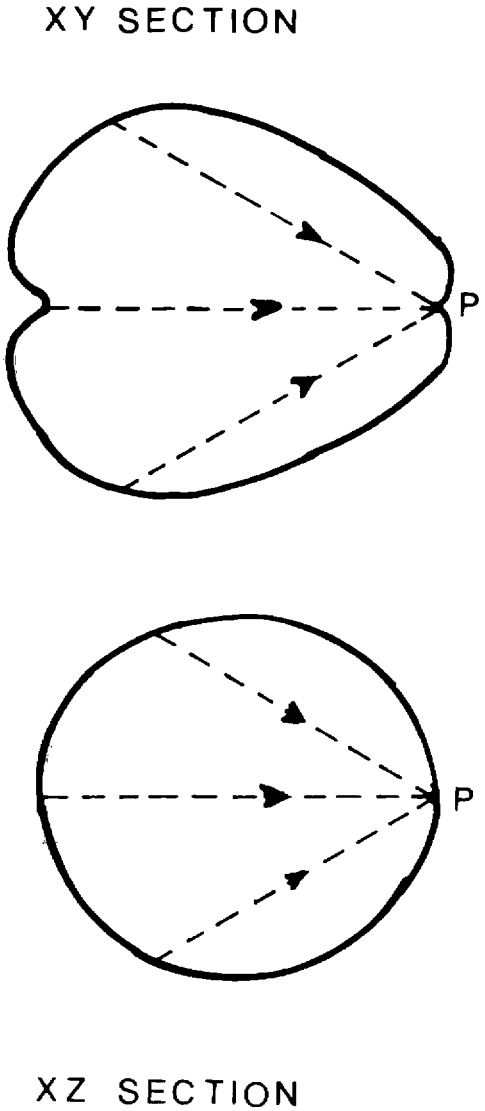

4. Qualitative Evaluation

4.1. Holes and Voids

It has been shown that under special geometrical conditions, holes and voids may be present in the workspace (Gupta and Roth 1981; Yang and Lee, 1983). *Holes* occur around the first axis and have an irregular shape in the axial cross-section. A simple example is the hole in a donut. *Voids* are internal empty spaces. Two types of voids are possible:

1. *Central voids* occur around the first axis and are like the core of an apple.
2. *Toroidal voids* or *noncentral voids* occur within the active workspace and are like the hollow part of a hollow ring.

The *generative process* for determining a workspace follows the sequence: $W_6(P)$ = point, $W_5(P)$ = circle, $W_4(P)$ = torus, $W_3(P)$ = complex solid of revolution, . . . , $W_1(P)$ = complex solid of revolution. The geometry of a torus is well understood. When a torus is revolved around an axis, a complex solid of revolution with holes and central and toroidal voids is generally obtained. Let us discuss the transformations of holes and voids when a complex solid of revolution $W_{k+1}(P)$ is revolved around the axis k to obtain another complex solid of revolution $W_k(P)$.

A hole changes into another hole if the axis k passes through the hole of workspace $W_{k+1}(P)$ without intersecting it. A hole is eliminated if the angle between the axes k and $k+1$ is small and the axis k does not pass through the hole. The hole becomes a central void if the angle between the axes k and $k+1$ is large and the axis k cuts the workspace $W_{k+1}(P)$, passing nearly centrally through the hole. The hole becomes a toroidal void if the angle between the axes k and $k+1$ is large and the axis k does not pass through the hole. Finally, the hole becomes both a central void and a toroidal void if the angle between the axes k and $k+1$ is large and the axis k cuts the workspace $W_{k+1}(P)$, passing off centered through the hole.

A central void changes into another central void if the axis k passes through it; otherwise, it is eliminated. A toroidal void becomes another toroidal void if the axes k and $k+1$ are nearly the same (i.e., small angle and distance). If the axis k passes through the toroidal void, then the toroidal void becomes a central void. If the axis k is outside of the workspace $W_{k+1}(P)$ then the toroidal void is eliminated. This also occurs when the angle between k and $k+1$ is large but the axis k does not lie outside of the workspace $W_{k+1}(P)$. These qualitative results are summarized in Table 1.

4.2. Number of Solutions

A six-degrees-of-freedom robot can have up to 32 possible solution sets of joint variable values to reach

Table 1. Transformations of Holes and Voids

In $W_{k+1}(P)$	Distance $(k, k+1)$	Angle $(k, k+1)$	Additional requirement relative $W_{k+1}(P)$	In $W_k(P)$
hole			k through hole, no intersections	hole
hole		small	k does not pass through the hole	solid
hole		large	k intersects, passes almost centrally through the hole	central void
hole		large	k does not pass through the hole	toroidal void
hole		large	k intersects, passes off-centered through the hole	central & toroidal void
central void			k passes through the central void	central void
central void			k does not pass through the central void	solid
toroidal void	small	small		toroidal void
toroidal void			k passes through toroidal void	central void
toroidal void			k is outside	solid
toroidal void		large	k is not outside	solid

the same end-effector position (Roth 1976; Duffy and Crane 1980). However, some of these solutions may not be physically attainable due to joint variable range limits, mechanical interference among the links, collisions with obstacles in the environment, etc. Therefore, from the point of view of task-related flexibility, the manipulator configuration should have a large number of solution sets. The disadvantage is that the complexity or difficulty of closed-form solutions increases as the number of possible solution sets increases. The increased amount of computation makes the control of the manipulator more difficult. Some specific examples of the multiplicity of solution sets are the *IBM* robot with two solutions, the *Stanford Arm* with four solutions, and the *Unimation Puma* and *Cincinnati-Milacron* T^3 with eight solutions.

A common arrangement involves a three-degrees-of-freedom positioning of the wrist point H, and a three-roll wrist with revolutes cointersecting at the wrist (or equivalent wrist configurations). In such an arrangement, there are up to four possible ways to position the wrist point H, and up to two possible ways to orient the tool tip point P with respect to the wrist point H. Thus there are up to eight possible solution sets for such an arrangement. For the three-degrees-of-freedom positioning of the wrist point H, there are eight combinations of revolutes and prismatics: PPP, PPR, PRP, RPP, PRR, RPR, RRP, RRR; there are 12 Denavit and Hartenberg parameters that define the corresponding geometry. Analytical details for these arrangements can be found in Pieper and Roth (1969) and Spanos and Kohli (1985) and in the known solutions for configurations such as *IBM, Unimation Unimates, Stanford Arm, Unimation Puma, Cincinnati-Milacron-Electric,* and *Bendix* (Pieper and Roth 1969; Duffy 1980; Gupta 1981; Paul 1981; Litvin and Parenti Castelli 1984).

We now present a method for deducing the number of solution sets for three-degrees-of-freedom positioning from the workspace theory. We will first consider

Fig. 4. A two-jointed robot (upper) and its kinematic inversion (lower).

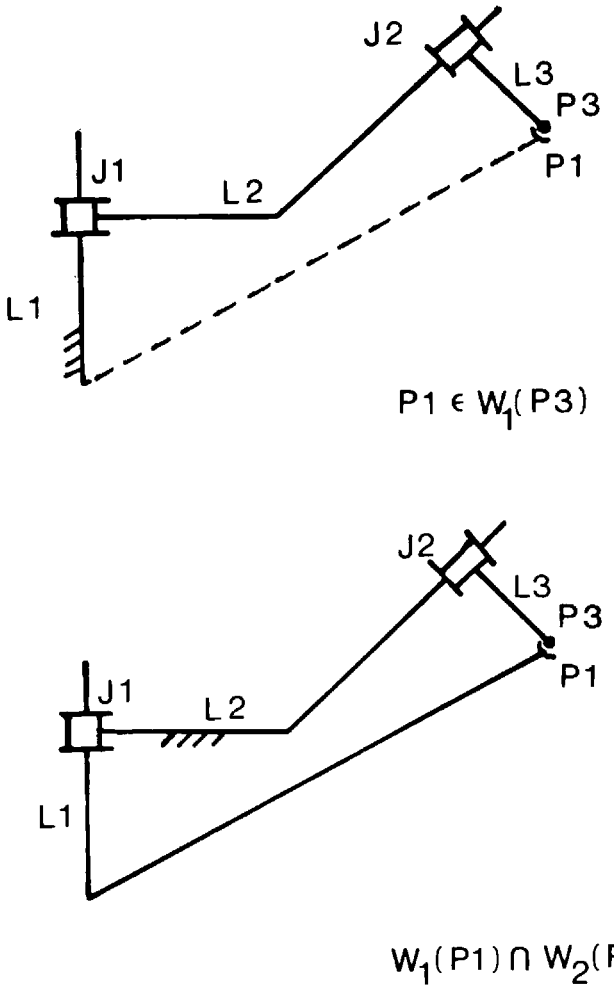

the two-revolute jointed chain in Fig. 4. The workspace $W_2(P)$ is a circle and $W_1(P)$ is a torus. Depending upon the link dimensions, the torus can take many different shapes (Fichter and Hunt 1975). We need to know in how many ways a point on the torus can be reached. The geometric argument is based upon a kinematic inversion with respect to link 2. This is done by temporarily fixing link 2 and freeing link 1. Interpreting point P on link 1 as P_1 and on link 3 as P_3, we can define the solution as the intersection of workspaces $W_2(P_3)$ and $W_1(P_1)$, both of which are circles. For the original manipulator, the corresponding question is: As the workspace $W_2(P_3)$, which is a circle, revolves around the axis 1, how many times does it pass through point P? The answer could be zero (P_1 is not in the workspace), one (circle $W_2(P_3)$ is generally oriented), or two (axes 1 and 2 are parallel or intersecting). These are the possible number of solution sets for the RR chain.

Fig. 5. Three-jointed positioning of the wrist point H.

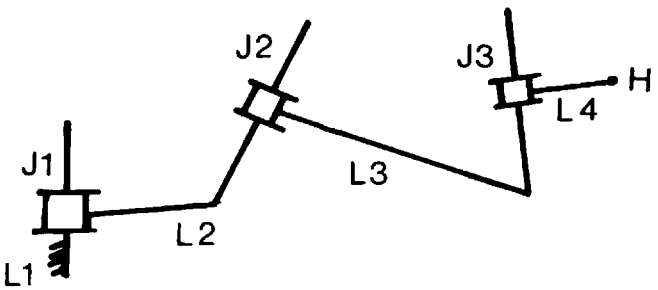

If the two-link chain consists of RP joints, then the workspace $W_2(P_3)$ is a line. As the workspace $W_2(P_3)$ goes around axis 1, it may pass through point P_1 the following number of times: zero (P_1 is not in the workspace), one (line $W_2(P_3)$ is generally oriented), or two (axes 1 and 2 are perpendicular). These are the possible number of solution sets for the RP chain.

If the two-link chain consists of PR joints, then the workspace $W_2(P_3)$ is a circle. As it is translated along axis 1, it may pass through the point the following number of times: zero (P_1 is not in the workspace), one (circle $W_2(P_3)$ is generally oriented), or two (axes 1 and 2 are perpendicular). These are the possible number of solution sets for the PR chain.

The situation becomes slightly more complex when a three-jointed chain is considered (Fig. 5). Let the joints be numbered 1 (base), 2, and 3 and point H on terminal link 4 be H_4 and on the base link be H_1. The method is applied in two steps.

The first step involves joints 2 and 3 only, and the above discussion dealing with two-jointed chains is directly applicable with axes numbers suitably interpreted. The number of times the circle $W_3(H_4)$ can pass through H_2 is determined. Thus there can be zero, one, or two possible ways in this step.

The second step involves all three joints. The workspace $W_2(H_4)$ is a torus in its general or special form. As the workspace $W_2(H_4)$ revolves around axis 1, it may pass through point H_1 the following number of times: zero (point H_1 is not in the workspace); two (general torus, special torus such as sphere or plane); or four (general torus).

Fig. 6. A 3R manipulator (upper), its workspace at joints J2 (middle) and J1 (lower). Zones of two and four solution sets are indicated in the workspace $W_1(H_4)$ at joint J1.

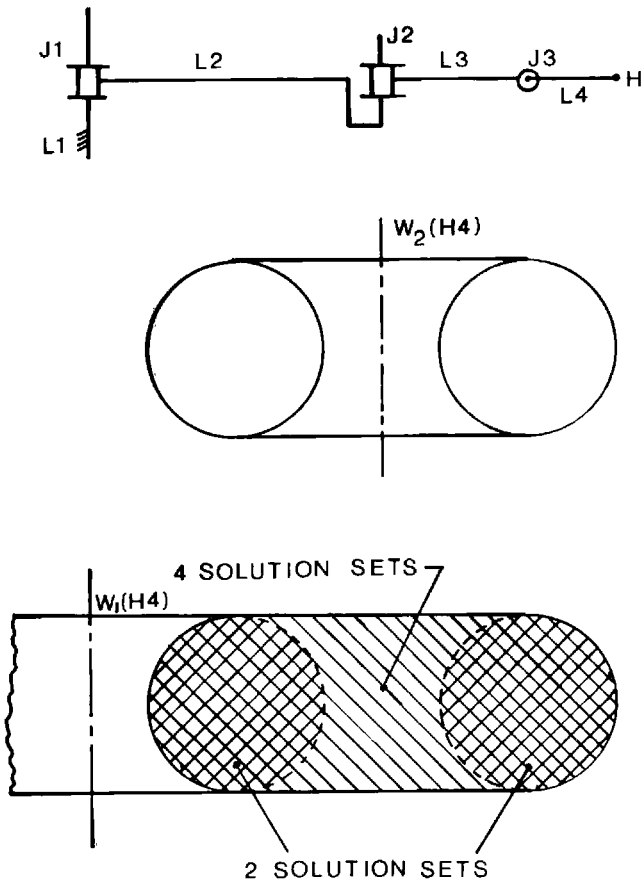

The number of solution sets for the three-jointed chain is obtained by multiplying the possible numbers of ways in the first and second steps. It may appear that there could be up to eight possible solution sets for the three-jointed chain, but this is incorrect. If a kinematic inversion with respect to link 2 is considered, i.e. link 2 is temporarily fixed and link 1 is free, then the solutions are given by the intersection of torus $W_2(H_4)$ and circle $W_1(H_1)$. Although the torus is a fourth order surface and the circle is a second order curve and one may expect up to eight possible intersections, there are at most four real solutions due to the circularity of the circle and torus. Thus the three-jointed chain for the positioning of the wrist point H has up to four possible solution sets, not eight.

For example, consider the R $\perp$ R $\perp$ P construction for spherical positioning. The workspace $W_3(H_4)$ is a line perpendicular to axis 2. As this line revolves around axis 2, it passes through a point H_2 twice. However, only one of these solutions is usable; the other solution would be impractical because it would involve sliding point H_4 through the prismatic joint and moving it to the other side of the second revolute. Next, the workspace $W_2(H_4)$, which is a plane containing the first revolute axis, is revolved around the first axis and it will pass through point H_1 twice. Thus, only two (not four) solution sets are usable in the spherical RRP construction. Examples of spherical construction are *Unimation Unimates* and *Bendix*. The above analysis is applicable with minor modifications to the RRP construction of the *Stanford Arm*.

As another example, consider the articulated R $\perp$ $R \parallel R$ construction of *Unimation Puma*. The workspace $W_3(H_4)$ is a circle that lies in a plane perpendicular to axis 2. When this circle is revolved around the axis, it passes through point H_2 twice. The workspace $W_2(H_4)$ is a circular plate whose plane is parallel to axis 1. When this plate is revolved around axis 1, it passes through point H_1 twice. Therefore, there are four (2×2) solution sets.

Another important observation is that the workspace $W_1(H_4)$ can be divided into zones with different numbers of possible solution sets. Let us consider the situation where the workspace $W_3(H_4)$ passes through the point H_2 only once. Then, as the torus $W_2(H_4)$ is moved with respect to the joint axis $J1$ (revolved if $J1$ is revolute, translated if $J1$ is prismatic), it may pass through the point H_1 zero or two or four distinct times. The actual number of solutions (product of 1 with 0 or 2 or 4) will depend upon the shape of the torus and the relative locations of point H_1 and torus $W_2(H_4)$. The workspace $W_1(H_4)$ therefore will contain transition boundaries where some of the otherwise distinct solutions coalesce into fewer solutions. A simple illustration with the $R \parallel R \perp R$ configuration is shown in Fig. 6. The zones where four and two distinct solutions exist, and the boundaries where three or one distinct solutions exist are shown in Fig. 6.

A similar argument when used for the $R \perp R \parallel R$ configuration of *Puma* indicates that four distinct solution sets exist throughout the interior of the workspace $W_1(H_4)$, and transition cases occur at the boundaries of the workspace $W_1(H_4)$.

These transition boundaries represent singular configurations of three-jointed positioning. When a three-

Fig. 7. Workspace of Cincinnati-Milacron T^3 manipulator with data in Table 2, Case I.

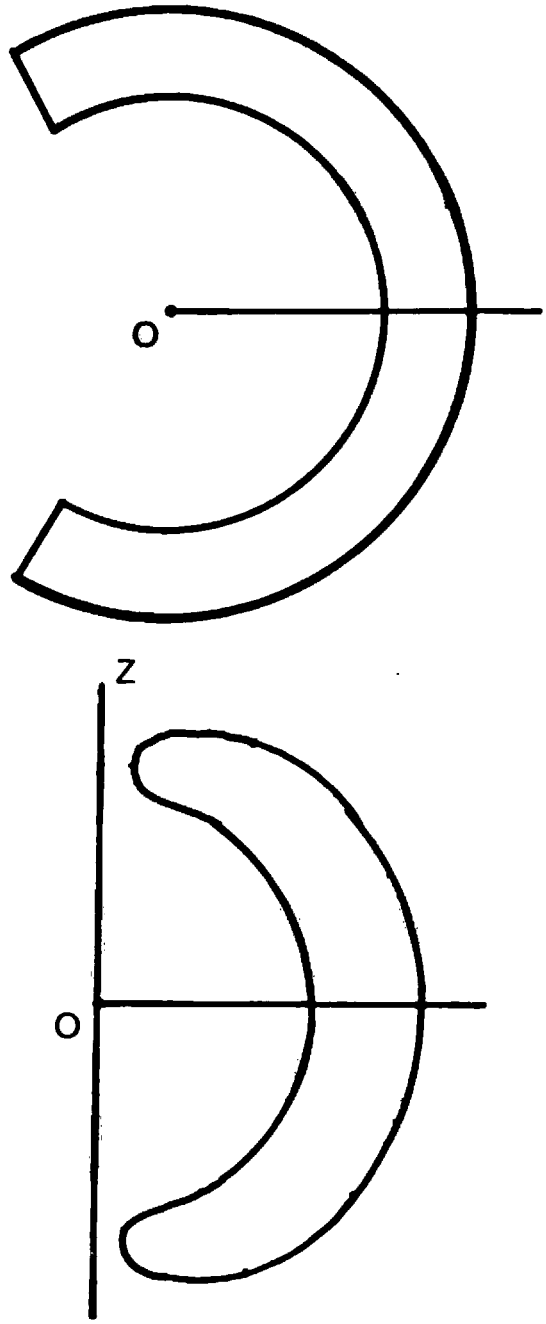

roll wrist with the last three cointersecting revolutes is added, then the primary (or dexterous) workspace of the six-degrees-of-freedom robot can be determined. It is clear that portions of the above-mentioned transition boundaries may lie within the dexterous workspace.

In a more general case, where this decoupling of position and orientation does not occur, it is also possible for manipulator singularities to exist within the dexterous workspace.

For other approaches to manipulator singularities, Hansen (1983), Litvin and Parenti Castelli (1984), and Spanos and Kohli (1985) should be consulted.

4.3. Joint Variable Ranges

The full ranges of 360-degree rotation at revolute joints and arbitrary travel at prismatic joints are not possible due to space and hardware limitations and mechanical interference among the links. When the joints have limited travel, both the magnitudes and mid-point placement of joint variable ranges affect the workspace significantly. Figures 7 and 8 show two workspaces of *Cincinnati-Milacron* T^3 configuration (Table 2), where the variable ranges are the same but the mid-point placements of the ranges are different (Cases I and II). One may therefore do a volumetric optimization of the workspace with respect to the limited variable ranges and mid-point placements of the ranges.

Alternately, the joint angle ranges and their mid-point placement may often be chosen to eliminate or reduce their influence upon the workspace. That is, the manipulator with full angle ranges and the one with limited angle ranges may have identical or nearly similar workspaces under certain conditions.

That this can be done at all is surprising, and the key is a judicious exploitation of the multiplicity of the solution sets. Let us discuss the examples shown in Fig. 9. In the first case, if joint 2 has full mobility but joint 3 has 180-degree mobility as shown, then the workspace $W_1(H)$ remains unchanged. The difference however is that while there are four (2×2) solution sets for the positioning of point H in the interior of the workspace when all joints have full mobility, there are only two (1×2) solution sets when joint 3 has 180-degree mobility as shown. If joint 3 has partial mobility greater than 180 degrees, then the workspace contains zones where 2 and 4 solution sets exist.

In the second case, if joint 2 has full mobility, then the joints 4 and 6 can have 180-degree mobility as shown without affecting the workspace $W_1(P)$. Likewise, if joint 1 has full mobility, then joints 3 and 5 can

Fig. 8. Workspace of Cincinnati-Milacron T^3 manipulator with data in Table 2, Case II.

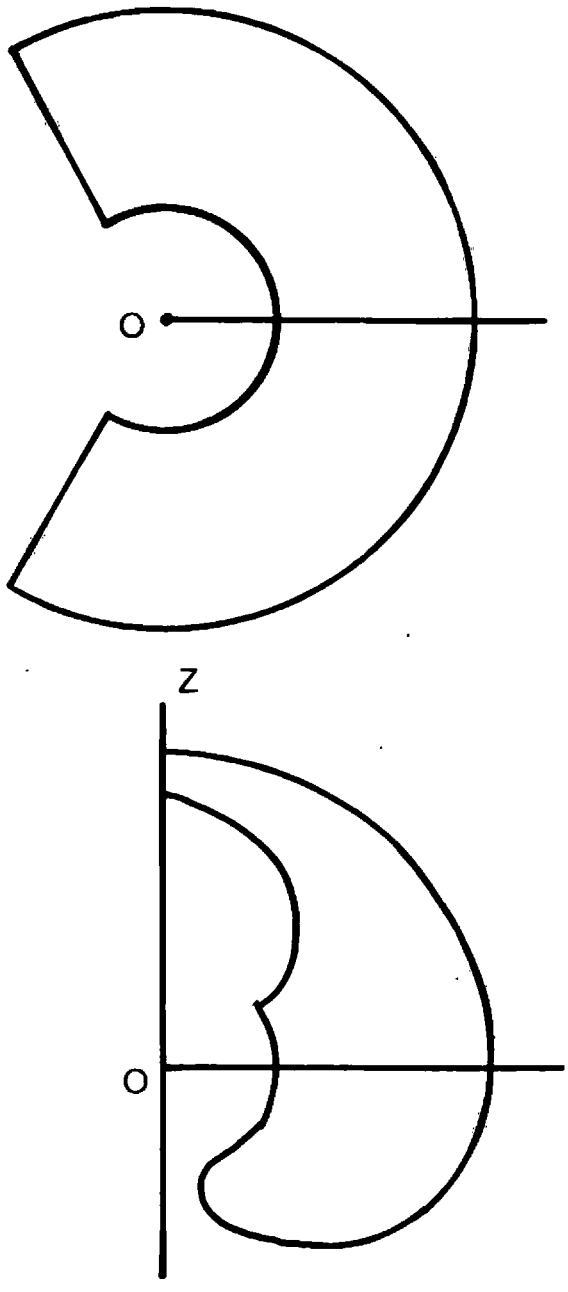

Fig. 9. Influence of joint angle ranges on manipulator workspace. Workspaces in above three examples are unchanged when the unmarked joints have full 360 degree ranges, while the marked joints have full 360 degree ranges or 180 degree ranges as indicated.

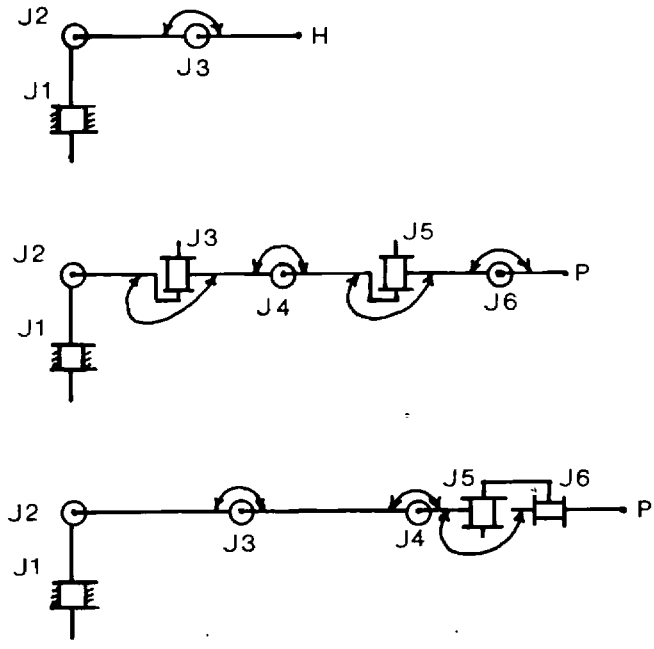

Table 2. Parameters for Cincinnati-Milacron T^3

					θ_i midpoint	
i	a_i	α	s_i	$\Delta\theta_i$	Case I	Case II
1	**0**	90°	0	240°	0	0
2	**40″**	0	0	90°	0	45°
3	**40″**	0	0	120°	0	−60°
4	**8″**	−90°	0	240°	0	0
5	**0**	90°	0	240°	0	90°
6	0	0	0	360°	0	0

have 180-degree mobility as shown without affecting the workspace $W_1(P)$.

In the third case, if joint 2 has full mobility, then joints 3 and 4 can have 180-degree mobility as shown without affecting the workspace $W_1(P)$. And if joint 1 has full mobility, then joint 5 can have 180-degree mobility as shown without affecting the workspace $W_1(P)$.

In general, if the workspace $W_{k+1}(P)$ is symmetric with respect to a plane through the axis of full mobility joint k, then some joints with indices higher than k can be restricted without influencing the workspaces $W_k(P)$.

5. Conclusions

Recent advances in the configuration synthesis of robots are presented. It is also shown how the work-

space theory can be used to further our understanding of biomanipulation, existence of holes and voids, multiple solution sets, and joint variable range effects.

6. Acknowledgments

Permission of the *Israel Journal of Technology*, Weizmann Science Press of Israel to republish this paper (final revision December 27, 1985) is gratefully acknowledged. This paper was first presented at the 18th Israel Conference on Mechanical Engineering, Haifa, June 27-28, 1984.

References

Denavit, J., and Hartenberg, R. S. 1955. A kinematic notation for lower pair mechanisms based on matrices. *ASME J. Applied Mechanics* 77:215-221.

Duffy, J. 1980. *Analysis of mechanisms and robot manipulators.* New York: Wiley-Interscience.

Duffy, J., and Crane, C. 1980. A displacement analysis of the general spatial 7 link 7R mechanism. *Mechanism and Machine Theory* 15:153-169.

Fichter, E. F., and Hunt, K. H. 1975. The fecund torus—its bitangent-circles and derived linkages. *Mechanism and Machine Theory* 10:167-176.

Freudenstein, F., Longman, R. W., and Chen, C. K. 1984. Kinematic analysis of robotic bevel gear trains. *ASME J. of Mechanisms, Transmissions, and Automation in Design* 106:371-375.

Gupta, K. C. 1981 (Dec. 7-9, Kansas City, Mo.). A note on position analysis of manipulators. *Proc. 7th Applied Mechanisms Conf.*, pp. 2.1-2.3. Also see: 1984. *Mechanism and Machine Theory* 19:5-8.

Gupta, K. C. 1985. Kinematic analysis of robotic bevel gear trains—discussion. *ASME J. of Mechanisms, Transmissions, and Automation in Design* 107:142-143.

Gupta, K. C., and Roth, B. 1981. Design considerations for manipulator workspace. *ASME Paper 81-DET-79.* Also see: 1982. *ASME J. of Mechanical Design* 104:704-711.

Hansen, J. A. 1983. Generation and evaluation of the workspace of a manipulator. Master's thesis, University of Illinois at Chicago.

Hansen, J. A., Gupta, K. C., and Kazerounian, S. M. K. 1983. Generation and evaluation of the workspace of a manipulator. *Int. J. Robotics Res.* 2:22-31.

Kumar, A., and Waldron, K. J. 1981. The workspace of a mechanical manipulator. *ASME J. Mechanical Design* 103:665-672.

Lin, P. N., and Duffy, J. 1982 (Aug. 15-19, San Diego). The mapping and structure of the workspace of robot manipulators with revolute and prismatic pairs. *Proc. ASME 2nd Int. Computer Eng. Conf.*, pp. 165-172.

Litvin, F. L., and Parenti Castelli, V. 1984 (Atlanta). Robot's manipulator: simulation and identification of configurations, execution of prescribed trajectories. *Proc. IEEE Int. Conf. Robotics*, pp. 34-44.

Paul, R. P. 1981. *Robot manipulators.* Cambridge: MIT Press.

Pieper, D. L., and Roth, B. 1969 (Warsaw). The kinematics of manipulators under computer control. *Proc. 2nd IFToMM Int. Congress on Theory of Machines and Mechanisms* 2:159-168.

Roth, B. 1976. Performance evaluation of manipulators from a kinematic viewpoint. *Performance Evaluation of Programmable Robots and Manipulators.* NBS #459. U.S. Govt. Printing Office, pp. 39-61.

Spanos, J., and Kohli, D. 1985. Workspace analysis of mechanical manipulators using polynomial discriminants. *ASME J. Mechanisms, Transmissions, and Automation in Design* 107:209-222.

Sugimoto, K., and Duffy, J. 1981. Determination of extreme distances of a robot hand—Part 1. *ASME J. Mechanical Design* 103:631-636.

Tsai, Y. C., and Soni, A. H. 1981 (Dec. 7-9, Kansas City, Mo.). The effect of link parameters on the working space of general 3R robot arms. *Proc. 7th Applied Mechanisms Conf.*, pp. 3.1-3.6.

Tsai, Y. C., and Soni, A. H. 1983. An algorithm for the workspace of a general N-R robot. *ASME J. Mechanisms, Transmissions, and Automation in Design* 105:52-57.

Yang, D. C. H., and Lee, T. W. 1982. Optimization of manipulator workspace. *Robotics Res. and Advanced Applications.* ASME Winter Annual Meeting, pp. 27-33.

Yang, D. C. H., and Lee, T. W. 1983. On the workspace of mechanical manipulators. *ASME J. Mechanisms, Transmissions, and Automation in Design* 105:70-77.